Zeitschrift für Physikalische Chemie, Bd. 212, S. 85–92 (1999)

Photoinduced Charge Injection from Vibronically Hot Excited Molecules of a Dye Sensitizer into Acceptor States of Wide-Bandgap Oxide Semiconductors

J.-E. Moser*, M. Wolf[1], F. Lenzmann and M. Grätzel

Laboratoire de Photonique et Interfaces, Institut de Chimie Physique,
Ecole Polytechnique Fédérale de Lausanne, CH-1015 Lausanne, Switzerland

(Received August 24, 1998; accepted December 10, 1998)

Interfacial electron transfer kinetics / Semiconductor dye-sensitization / Nanocrystalline oxides / Hot excited states reactions / Ultrafast phenomena

cis-$Ru^{II}(dcbpy)_2(NCS)_2$ complex was adsorbed onto transparent nanoporous films of TiO_2, Nb_2O_5, Ta_2O_5 and ZrO_2. On the last three materials, the $v' = 0$ energy level of the lowest MLCT excited state of the dye lies way below the bottom of the conduction band of the solid, where hardly any electron acceptor state is available. The absolute quantum yield for charge injection from the molecular sensitizer into these oxide semiconductors was measured by fast transient absorbance spectroscopy and was found to depend strongly upon the excitation photon energy. This observation provides the first reported evidence that interfacial electron transfer can indeed occur prior to nuclear relaxation of the sensitizer's excited state. Implications of this finding for the theoretical modeling of ultrafast electron injection kinetics are discussed.

Introduction

Unlike for charge transfer reactions in homogeneous media, electron transfer dynamics at the solid/adsorbate interface is still flimsily understood. Charge injection from an electronically excited dye moelcule (S*) into a continuum of acceptor states constituting the conduction band of a solid (SC) is a model interfacial electron transfer reaction. Besides its fundamental interest, research in this field is strongly motivated by numerous

* Corresponding author. Fax +41 21 693 4111; E-mail: je.moser@epfl.ch
[1] Present address: Leclanché S.A., R&D Department, CH-1400 Yverdon, Switzerland.

practical applications. Dye-sensitization of wide bandgap semiconductors via photoinduced electron injection is indeed at the basis of technologically important processes in photography and xerography. In the last decade, redox sensitization of oxide nanoparticles has found an additional relevance in the photoelectrochemical solar energy conversion [1].

The simplest kinetic model describing the electron injection as a non-adiabatic radiationless process is derived from Fermi's Golden Rule. For a large number of accessible acceptor levels, the summation over all the terms of the Franck-Condon factor approaches the value 1. In this case, the expression of the FC factor reduces to the unweighted density of final states [2, 3]:

$$k_i = \frac{2\pi}{\hbar} \cdot |H|^2 \cdot \frac{1}{h\omega} \cdot n_a \,. \tag{1}$$

In Eq. (1), the actual density of final states is approximated by the reciprocal energy level spacing $1/h\omega$ of the dye cation S^+ oscillator, multiplied by a factor n_a accounting for the density of empty electronic states available in the solid. Above the flatband energy level, the density of states in the conduction band of a semiconductor is usually very high and $n_a \cong 1$. Below the band edge, empty trap states are often present, whose density decreases gradually at lower energies ($n_a \rightarrow 0$).

Eq. (1), however, can only be used when the electron transfer process takes place from a single prepared excited state of the sensitizer. In the general case, absorption of photons, whose energy $h\nu$ is larger than the electronic excitation energy $\Delta E_{0,0}$ of the dye, leads to the population of higher vibronic levels of the molecule (Eq. (2)). Relaxation of those vibrationally excited intramolecular states (Eq. (3)) and of the whole system along the classical reaction coordinate is expected to compete with the electron transfer process (Eq. (4)) [4]. In these conditions, the electronic coupling $|H|$ between the donor and acceptor states becomes a time- and excitation wavelength-dependent function and cannot be accessed easily.

$$S|SC + h\nu\,(>\Delta E_{0,0}) \rightarrow S^*(v' > 0)|SC \tag{2}$$

$$S^*(v' > 0)|SC \rightarrow S^*(v' = 0)|SC + \nabla \qquad k_r \tag{3}$$

$$S^*(v' > 0)|SC \rightarrow S^+|(e^-)SC \qquad k_i' \tag{4}$$

$$S^*(v' = 0)|SC \rightarrow S^+|(e^-)SC \qquad k_i \tag{5}$$

$$S^*(v' = 0)|SC \rightarrow S|SC + h\nu' + \nabla \qquad \Sigma k_d \tag{6}$$

$$S^+|(e^-)SC \rightarrow S|SC \qquad k_b \tag{7}$$

Recently, electron injection processes for efficient redox sensitizers of TiO_2 were reported to take place in the femtosecond regime [5–8]. The vibrational relaxation of the dye excited state, on the other hand, is expected to occur within a few picoseconds ($k_r \cong 10^{12}\ s^{-1}$). Observed injection rate

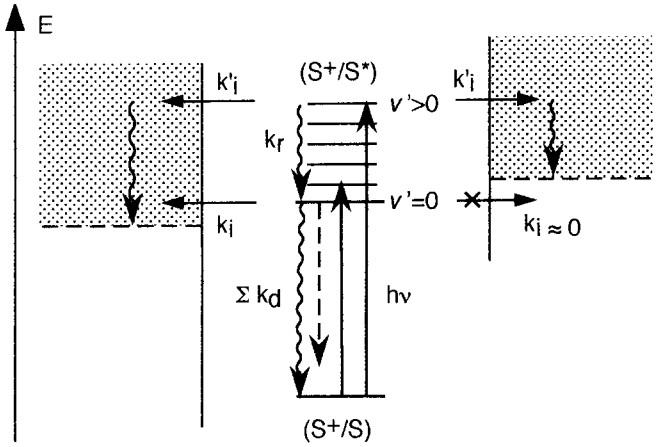

Fig. 1. Energy scheme for photoinduced electron transfer from the excited state S* of a dye-sensitizer to the conduction band acceptor levels of a semiconductor. In favorable thermodynamic conditions (left side), injection quantum yield is controlled by the competition between the ET process (k_i, k_i') and the deactivation of the dye excited state (Σk_d). When the $v' = 0$ level of S* lies below the conduction band edge (right side), only hot vibronically excited states formed upon excitation at shorter wavelengths are thermodynamically able to inject into the solid. In the latter case, injection quantum yield is controlled by the kinetic competition between charge injection (k_i') and nuclear relaxation (k_r).

constants of the order of 10^{13} s^{-1} thus certainly preclude complete thermalization of S* to the $v' = 0$ level prior to the reaction, and suggest that charge transfer can occur directly from vibrationally hot ($v' > 0$) excited sensitizer molecules (Fig. 1).

In favorable thermodynamic conditions, where the lowest electronic excited state energy level of the sensitizer lies above the bottom edge of the conduction band, charge injection competes kinetically only with the decay of the sensitizer's excited state. Hence, for dyes that are characterized by emission lifetimes τ_f of the order of one nanosecond ($\Sigma k_d \cong 10^9$ s^{-1}), interfacial electron transfer rate constant of the order of $k_i \geq 10^{11}$ s^{-1} suffices to ensure high injection quantum yields $\Phi_i = k_i/(k_i + 1/\tau_f) \cong 1$. In the opposite case, the $v' = 0$ level of the electronically excited state of the dye lies below the bottom edge of the conduction band of the semiconductor, where the density of available acceptor states is small. In these conditions, charge injection from the vibrationally relaxed excited molecules of the sensitizer is either slow or unfeasible. However, if electron injection from a hot vibronic excited state of the dye is able to compete successfully with its nuclear relaxation ($k_i' \geq k_r$), charge injection should become possible for higher excitation photon energy, and an excitation wavelength dependence of the quantum yield $\Phi_i = k_i'/(k_i' + k_r)$ would be expected.

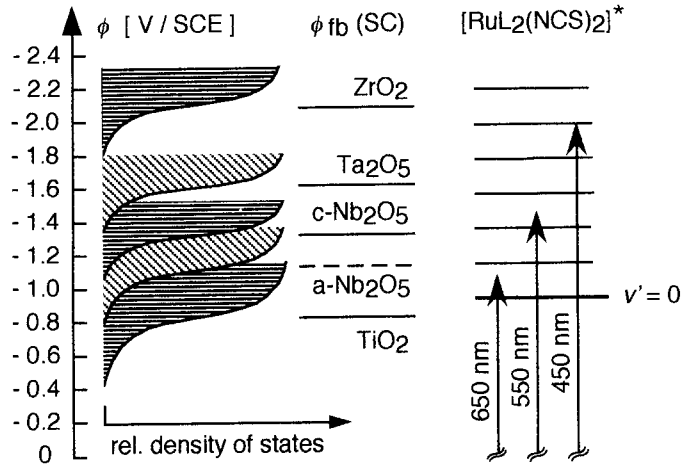

Fig. 2. Energy scheme for $Ru^{II}(dcbpy)_2(NCS)_2$ dye sensitizer adsorbed on various oxide semiconductors. Molecular levels are based on the values of the oxidation potential of the complex: $\phi^0(S^+/S) = +0.86$ V/SCE and excitation energy $\Delta E_{0,0} = 1.85$ eV [9]. The flatband potentials ϕ_{fb}(SC) of the different solid materials were estimated by monitoring the optical absorption at $\lambda = 900$ nm of transparent nanoporous electrodes in propylene carbonate as a function of applied potential.

Experiments, results and discussion

The *cis*-[bis(4,4′-dicarboxy-2,2′-bipyridyl)bis(thiocyanato)]ruthenium(II) complex is an efficient redox sensitizer of titanium dioxide. Upon irradiation by visible light, the adsorbed dye has been found to inject an electron into the semiconductor with a quantum yield approaching unity [9]. Ultrafast laser flash photolysis applied to dye-sensitized, transparent, nanocrystalline TiO_2 films show that electron injection from the MLCT excited state of the Ru-complex into the conduction band of the solid occurs within the femtosecond/picosecond timescale [7, 8]. This kinetics appears to be independent of the excitation photon energy, and the medium [8].

Nanoporous transparent layers (thickness 2–6 μm) of Nb_2O_5, in both amorphous and highly crystalline forms, as well as nanocrystalline Ta_2O_5 films were prepared on conductive glass substrate using hydrothermal procedures [10]. Mesoscopic TiO_2 and ZrO_2 films (thickness 8 μm) were prepared as previously reported [9]. The flatband potential and relative density of charge carriers in all five different types of oxide semiconductors were estimated from the measure of the optical absorbance at 900 nm of the naked electrodes under potentiostatic control [11]. The flatband energy of amorphous (a-Nb_2O_5) and crystalline (c-Nb_2O_5) niobia, of tantalum pentoxide (Ta_2O_5) and zirconia (ZrO_2) was found in dry propylene carbonate

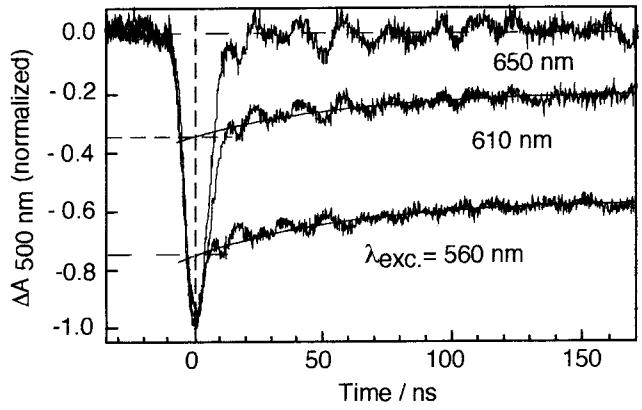

Fig. 3. Transient absorbance changes observed at λ = 500 nm upon ns laser excitation (pulse duration: 5 ns, fluence: $\leq$ 1 mJ/cm^2) of a dye-sensitized nanocrystalline layer of c-Nb_2O_5 in pure propylene carbonate. The absolute injection quantum yield is obtained from these bleaching signals and corresponds to the ratio of the absorbance change at longer time scale (20 ns $<$ 1 $<$ 150 ns), extrapolated to time zero, over the initial absorbance decrease observed upon laser excitation of the dye.

(0.2 M TBA triflate) to be 0.2, 0.4, 0.7 and 1.1 eV higher than that of TiO_2, respectively. As a consequence, the $v' = 0$ level of the MLCT excited state of the adsorbed $Ru^{II}(dcbpy)_2(NCS)_2$ dye lies below the bottom edge of the conduction band of these materials (Fig. 2).

All five different electrodes were sensitized by adsorption of the complex dye and subjected to flash photolysis (pulse duration: 5 ns, repetition rate: 30 Hz) in pure propylene carbonate. The laser excitation wavelength was tuned by use of an optical parametric oscillator between λ = 450 nm and 680 nm. The fluence per laser pulse was adjusted between 0.1 mJ/cm^2 (at 530 nm) and 1 mJ/cm^2 (at 680 nm) in order to produce bleaching signals of approximately the same amplitude at all excitation wavelengths. In these conditions, less than 1% of the adsorbed dye molecules were excited by each pulse. Monitoring of the sensitizer's ground state bleaching signal upon nanosecond laser flash photolysis of the Ru(II) complex clearly showed a biphasic kinetic behavior. Excited dye molecule that do not inject into the solid produce a recovery of the ground-state absorption within 15 ns (Eq. (6)). On the other hand, the dye cation S^+, produced by the photoinduced electron transfer process, recaptures the injected electron (Eq. (7)) in the microsecond time domain [12]. Both kinetic steps, whose rate constants differ by ca. two orders of magnitude, are easily separated. Quantitative evaluation of their respective amplitudes allows the determination of the absolute injection quantum yield Φ_i at any excitation wavelength, independently of the absorption spectrum of the dye (Fig. 3).

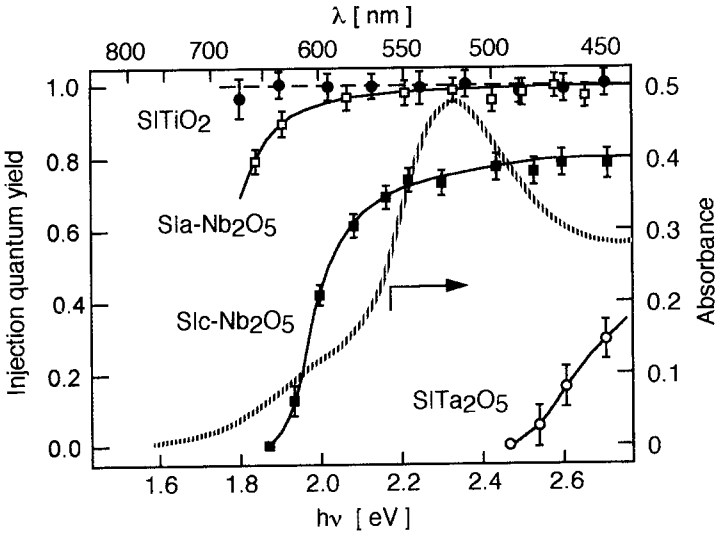

Fig. 4. Dependence of electron injection quantum yield Φ_i obtained for various dye-sensitized semiconductors upon excitation photon energy $h\nu$. Experimental conditions are given in the text. The ground state absorption spectrum of the dye S ≡ Ru^{II}-$(dcbpy)_2(NCS)_2$ is displayed for direct comparison (hatched line).

Results reported on Fig. 4 show a strong excitation wavelength dependence of Φ_i for dye sensitized c-Nb_2O_5 between λ = 650 nm, the onset of injection, and 500 nm, where the charge transfer quantum yield reached a plateau value of ~0.75. This yield reflects the kinetic competition between interfacial electron transfer and vibrational relaxation of the excited state. The maximum value obtained thus indicates that the injection rate constant k_i' must be here of the same order of magnitude than k_r ($\cong 10^{12}$ s^{-1}). Measurements conducted under identical conditions with dye-sensitized TiO_2 gave an injection quantum yield close to unity that was independent of the excitation wavelength. On amorphous Nb_2O_5, whose flatband potential is intermediate between those of TiO_2 and c-Nb_2O_5, the injection onset is shifted to the red by approximately 0.2 eV compared to nanocrystalline niobia. In this case, the quantum yields obtained at $\lambda \leq$ 600 nm reach a plateau value close to unity. On tantalum pentoxide, the injection onset is found in the blue at λ = 480 nm. The shift of the electron injection onset by +0.6 eV for Ta_2O_5 compared to c-Nb_2O_5 is larger than the energy difference measured between the positions of the respective conduction band edges of both materials (0.3 eV) and should probably be related to a lower density of sub-bandgap electronic states in tantalum pentoxide. Finally, in accord-

ance to the energy scheme of Fig. 2, no charge injection was observed for $Ru^{II}(dcbpy)_2(NCS)_2$ adsorbed on ZrO_2 up to an excitation photon energy of 2.7 eV.

These observations of an excitation wavelength dependence of the charge injection process are the first reported evidence that photoinduced electron transfer from a molecular electronic excited state to a continuum of acceptor levels can indeed compete kinetically with vibrational relaxation of the S* donor. This competition precludes in general the use of the simplified model depicted by Eq. (1). The rather slow growth of the quantum yield above the energy onset is observed moreover to map the density of acceptor states in the solid that are present below the conduction band edge, and shows that the factor n_a cannot be neglected in general.

However, in conditions where the injection quantum yield is unity ($k_i' \gg k_r$) and electron transfer takes place to the conduction band of the solid ($n_a \cong 1$), the occurrence of the injection process from a single prepared state $S^*(v' > 0)$ validates the simple model of Eq. (1) and allows to estimate the electronic coupling matrix element $|H|$. By admitting $\bar{w} \leq 1500\ cm^{-1}$, a value of $|H| \leq 154\ cm^{-1}$ ($\cong 0.7$ kT) is extracted from the rate constant $k_i = 2 \cdot 10^{13}\ s^{-1}$ obtained typically for $Ru^{II}(dcbpy)_2(NCS)_2$-sensitized nanocrystalline TiO_2. Although the value obtained for $|H|$ is here probably overestimated, it corresponds to a rather strong electronic coupling and suggests the electron injection rate could have reached the adiabatic limit.

Acknowledgements

The authors are grateful to J. R. Durrant, Y. Tachibana and S. A. Haque (Imperial College, London) for fruitful discussions and for sharing experimental results prior to publication. This work was supported by the Swiss National Science Foundation.

References

1. A. Hagfeldt and M. Grätzel, Chem. Rev. **95** (1995) 49.
2. J. M. Lanzafame, S. Palese, D. Wang, R. J. D. Miller and A. A. Muenter, J. Phys. Chem. **98** (1994) 11020.
3. R. J. D. Miller, G. L. McLendon, A. J. Nozik, W. Schmickler and F. Willig, *Surface Electron Transfer Processes*, VCH Publishers, New York 1995, Chapter 5.
4. Y. H. Meyer and P. Plaza, Chem. Phys. **200** (1995) 235.
5. J. E. Moser, P. Bonhôte and M. Grätzel, Coord. Chem. Rev. **171** (1998) 245.
6. a) J. M. Rehm, G. L. McLendon, Y. Nagasawa, K. Yoshihara, J. E. Moser and M. Grätzel, J. Phys. Chem. **100** (1996) 9577; b) B. Burfeindt, T. Hannapel, W. Storck and F. Willig, J. Phys. Chem. **100** (1996) 16463; c) N. J. Cherepy, G. P. Smestad, M. Grätzel and J. Z. Zhang, J. Phys. Chem. B **101** (1997) 10990; d) R. J. Ellingson, J. B. Asbury, S. Ferrere, H. N. Ghosh, J. R. Sprague, T. Lian and A. J. Nozik, J. Phys. Chem. B **102** (1998) 6455; e) H. N. Gosh, J. B. Asburry and T. Lian, J. Phys. Chem. B **102** (1998) 6482.

7. Y. Tachibana, J. E. Moser, M. Grätzel, D. R. Klug and J. R. Durrant, J. Phys. Chem. **100** (1996) 20056.
8. J. R. Durrant, Y. Tachibana, I. Mercer, J. E. Moser, M. Grätzel and D. R. Klug, Zeit. Phys. Chem., this issue.
9. M. K. Nazeeruddin, A. Kay, J. Rodicio, R. Humphry-Baker, E. Müller, P. Liska, N. Vlachopoulos and M. Grätzel, J. Am. Chem. Soc. **115** (1993) 6382.
10. a) M. Wolf, Ph.D. thesis, EPF Lausanne, 1998; b) D. D. Filho, P. P. Filho, U. Werner and M. A. Aegerter, J. Sol-Gel Sci. Technol. **8** (1997) 735.
11. G. Rothenberger, D. Fitzmaurice and M. Grätzel, J. Phys. Chem. **96** (1992) 5983.
12. a) J. E. Moser, Solar Energy Mater. Solar Cells **38** (1995) 343; b) S. A. Haque, Y. Tachibana, D. R. Klug and J. R. Durrant, J. Phys. Chem. B **102** (1998) 1745; c) J. E. Moser, D. Noukakis, U. Bach, Y. Tachibana, D. R. Klug, J. R. Durrant, R. Humphry-Baker and M. Grätzel, J. Phys. Chem. B **102** (1998) 3649.